EUKARYOTIC CELL, Nov. 2007, p. 2072–2080 Vol. 6, No. 11
1535-9778/07/$08.00+0 doi:10.1128/EC.00246-07

Multiple Modes of Chromatin Configuration at Natural Meiotic Recombination Hot Spots in Fission Yeast[▽]

Kouji Hirota,[1,2]* Walter W. Steiner,[3] Takehiko Shibata,[2] and Kunihiro Ohta[1,2]

Department of Life Sciences, Graduate School of Arts and Sciences, The University of Tokyo, Komaba 3-8-1, Meguro-ku, Tokyo 153-8902, Japan[1]; Shibata Distinguished Senior Scientist Laboratory, RIKEN Discovery Research Institute, Wako-shi, Saitama 351-0198, Japan[2]; and Department of Biology, P.O. Box 2032, Niagara University, Lewiston, New York 14109[3]

Received 6 July 2007/Accepted 25 August 2007

The *ade6-M26* meiotic recombination hot spot of fission yeast is defined by a cyclic AMP-responsive element (CRE)-like heptanucleotide sequence, 5′-ATGACGT-3′, which acts as a binding site for the Atf1/Pcr1 heterodimeric transcription factor required for hot spot activation. We previously demonstrated that the local chromatin around the *M26* sequence motif alters to exhibit higher sensitivity to micrococcal nuclease before the initiation of meiotic recombination. In this study, we have examined whether or not such alterations in chromatin occur at natural meiotic DNA double-strand break (DSB) sites in *Schizosaccharomyces pombe*. At one of the most prominent DSB sites, *mbs1* (*m*eiotic *b*reak *s*ite 1), the chromatin structure has a constitutively accessible configuration at or near the DSB sites. The establishment of the open chromatin state and DSB formation are independent of the CRE-binding transcription factor, Atf1. Analysis of the chromatin configuration at CRE-dependent DSB sites revealed both differences from and similarities to *mbs1*. For example, the *tdh1*$^+$ locus, which harbors a CRE consensus sequence near the DSB site, shows a meiotically induced open chromatin configuration, similar to *ade6-M26*. In contrast, the *cds1*$^+$ locus is similar to *mbs1* in that it exhibits a constitutive open configuration. Importantly, Atf1 is required for the open chromatin formation in both *tdh1*$^+$ and *cds1*$^+$. These results suggest that CRE-dependent meiotic chromatin changes are intrinsic processes related to DSB formation in fission yeast meiosis. In addition, the results suggest that the chromatin configuration in natural meiotic recombination hot spots can be classified into at least three distinct categories: (i) an Atf1-CRE-independent constitutively open chromatin configuration, (ii) an Atf1-CRE-dependent meiotically induced open chromatin configuration, and (iii) an Atf1-CRE-dependent constitutively open chromatin configuration.

Eukaryotic chromosomal DNA is compacted with histones and other proteins to form chromatin, which helps in efficient storage of genetic information. However, this prevents many DNA-associated processes, such as transcription, replication, repair, and recombination, from accessing the DNA template (38). Homologous recombination contributes to gaining genetic diversity in the next generation as well as proper segregation of homologous chromosomes in meiosis. Meiotic recombination is a highly regulated process, with some loci that are elevated (hot spots) or suppressed (cold spots) (15, 18, 22, 34).

In the distantly related budding and fission yeasts *Saccharomyces cerevisiae* and *Schizosaccharomyces pombe*, meiotic recombination hot spots are closely associated with sites of DNA double-strand breaks (DSBs), which are introduced by Spo11 (or its ortholog in *S. pombe*, Rec12) and are required for initiation of recombination (7, 22, 28, 30). Elevated sensitivity of chromatin to micrococcal nuclease (MNase) is found at meiosis-specific hot spots in both budding and fission yeasts (17, 21, 39).

The *ade6-M26* hot spot of fission yeast is the only reported eukaryotic hot spot whose essential nucleotide sequence, 5′-ATGACGT-3′, has been precisely defined. The *M26* hot spot confers a meiosis-specific elevation of recombination of up to 20-fold compared with other *ade6* alleles (e.g., *ade6-M375*) (8, 23, 25). The *ade6-M26* allele is a single G/T transversion at the 5′ end of the *ade6* coding region (23, 31). This mutation creates a nonsense codon and cyclic AMP-responsive element (CRE)-like heptanucleotide sequence. The heptamer acts as a binding site for the Atf1/Pcr1 (also called Mts1/Mts2 or Gad7/Pcr1) heterodimeric transcription factor, which is required for hot spot activation (14, 35). We have demonstrated that local chromatin with the *M26* sequence motif becomes more sensitive to MNase in the early stage of meiosis, suggesting active chromatin remodeling around *M26* (17). Furthermore, we have shown that Atf1 facilitates such chromatin remodeling (40).

Although the molecular basis of chromatin remodeling in *ade6-M26* has been analyzed, it remained unclear whether a similar mechanism occurs at natural hot spots of recombination. Recently, it was demonstrated that natural meiotic DSB sites defined by CRE-like sequences are present in the *S. pombe* genome and that one of the prominent DSB sites, the *cds1*$^+$ locus, is a meiotic recombination hot spot (29).

Moreover, Smith and colleagues analyzed natural DSBs in the *S. pombe* genome and identified the prominent meiotic DSB sites in chromosome I (1, 42). One such prominent DSB site, the *mbs1* locus (*m*eiotic *b*reak *s*ite 1), consists of clusters

* Corresponding author. Mailing address: Department of Life Sciences, Graduate School of Arts and Sciences, The University of Tokyo, Komaba 3-8-1, Meguroku, Tokyo 153-8902, Japan. Phone and fax: 81-3-5465-8834. E-mail: khirota@postman.riken.jp.

▽ Published ahead of print on 7 September 2007.

TABLE 1. *S. pombe* strains used in this study

Strain	Genotype
PKH50	*h*$^-$ *ade6-M26 rad50s pat1-114 ura4-D18 rec12-Flag:KanMX*
PKH52	*h*$^-$ *ade6-M26 rad50s pat1-114 ura4-D18 rad32-Flag:KanMX*
PKH118	*h*$^+$ *ade6-M26 rec12::ura4 rad50s pat1-114 ura4-D18 leu1-32*
PKH138	*h*$^+$ *ade6-M26 pat1-114 rad50s ura4-D18*
PKH160	*h*$^+$ *ade6-M26 pcr1::his3 pat1-114 rad50s his3-D1*
PKH163	*h*$^+$ *ade6-M26 aft1::ura4 pat1-114 rad50s ura4-D18 his3-D1*
PKH338	*h*$^-$ *ade6-M375 rad50s pat1-114 rec12-Flag:KanMX leu1-32*
PKH339	*h*$^-$ *ade6-M375 rad50s pat1-114 rad32-Flag:KanMX leu1-32*
D12	*h*$^+$/*h*$^-$ *ade6-M26/ade6-M26 rec12::ura4*$^+$*/rec12::ura4*$^+$ *ura4-D18/ura4-D18 his5-303/+ leu1-32/+*
D20	*h*$^+$/*h*$^-$ *ade6-M26/ade6-M26 his5-303/+ leu1-32/+*
D55	*h*$^+$/*h*$^-$ *ade6-M26/ade6-M26 rec7::ura4*$^+$*/rec7::ura4*$^+$ *ura4-D18/ura4-D18 his5-303/+ leu1-32/+*
D66	*h*$^+$/*h*$^-$ *ade6-M26/ade6-M26 mei4::ura4*$^+$*/mei4::ura4*$^+$ *ura4-D18/ura4-D18 his5-303/+ leu1-32/+*
D67	*h*$^+$/*h*$^-$ *ade6-M26/ade6-M26 rec6::ura4*$^+$*/rec6::ura4*$^+$ *ura4-D18/ura4-D18 his5-303/+ leu1-32/+*
D68	*h*$^+$/*h*$^-$ *ade6-M26/ade6-M26 rec8::ura4*$^+$*/rec8::ura4*$^+$ *ura4-D18/ura4-D18 his5-303/+ leu1-32/+*
D69	*h*$^+$/*h*$^-$ *ade6-M26/ade6-M26 rec10::ura4*$^+$*/rec10::ura4*$^+$ *ura4-D18/ura4-D18 his5-303/+ leu1-32/+*
D70	*h*$^+$/*h*$^-$ *ade6-M26/ade6-M26 rec15::ura4*$^+$*/rec15::ura4*$^+$ *ura4-D18/ura4-D18 his5-303/+ leu1-32/+*
WSP779	*h*$^+$/*h ade6-M26/ade6-M26 atf1::ura4/atf1::ura4 his3-D1/his3-D1 leu1-32/leu1-32 ura4D18/ura4D18*

of DSBs and is a meiotic recombination hot spot (2). However, the correlation of DSB formation and the chromatin structure has not been fully elucidated. In this study, we analyzed the chromatin structure of natural meiotic DSB sites, demonstrating that meiotic DSBs are introduced around the regions where the chromatin configuration is either constitutively open or induced to become open during meiosis. These results demonstrate that the CRE-mediated chromatin remodeling coupled to DSB formation is one of the intrinsic and general properties of natural CRE-related hot spots.

MATERIALS AND METHODS

Fission yeast strains, culture methods and media. The *S. pombe* strains used in this study are listed in Table 1. General genetic procedures were carried out as described previously (9). To induce meiosis using diploid *S. pombe* strains, cells were cultured in MM medium (12) to ~1 × 10^7 cells/ml. Cells were harvested and washed with distilled H_2O twice then transferred to MM medium lacking nitrogen (NH_4Cl) to induce meiosis. For synchronous meiosis, a *pat1-114* mutant strain was cultured in MM medium containing nitrogen at 25°C, transferred to MM medium lacking nitrogen at a density of 0.6 × 10^7 cells/ml, and cultured further for 20 h to arrest the cell cycle at the G_1 phase. An equal volume of MM-NH_4Cl (0.1%) medium was warmed at 37°C and added to the G_1 phase-arrested cell culture. The culture temperature was then raised to 34°C to induce meiosis.

For the construction of strains expressing proteins with epitope tags, we followed a standard integration method using the integration vector int4, which was derived from int2 (10) by replacing the green fluorescent protein open reading frame (ORF) with Flag. The diploid strains expressing fusion protein (Rec12-Flag or Rad32-FLAG) can normally form viable spores, indicating that the fusion proteins are functional.

Northern blot analysis. Total RNA was prepared from *S. pombe* cells by a method described elsewhere (5). For the Northern blot analysis, 10 μg of total RNA was denatured with formamide, separated on 1.5% agarose gels containing formaldehyde (24), and blotted on a charged nylon membrane (BioDyne B membrane; Pall, NY). The probe to detect the *cds1*$^+$ transcript was the same probe used for Fig. 7. The probe to detect the *tdh1*$^+$ transcript was prepared from a PCR-amplified DNA fragment using a random-priming kit (GE Healthcare, Little Chalfont, United Kingdom). The DNA fragment was amplified from *S. pombe* genomic DNA by PCR using the primer set ACGGTTTCGGTCGTA TTGGA and CATGAGACCCTCCTCGATAC.

Chromatin analysis. Isolation of crude chromatin from cells and digestion with MNase were performed as described by Mizuno et al. (17) with slight modifications as described bellow. The samples of chromatin were prepared from a fixed amount of cells (0.5 g [wet weight]). These cells were suspended in preincubation buffer (0.7 M β-mercaptoethanol, 3 mM EDTA, 20 mM Tris-HCl [pH 8.0]), incubated at 30°C for 10 min, and washed once with 5 ml of ice-cold wash buffer (1.0 M sorbitol, 10 mM EDTA). Cells were centrifuged and resuspended in 2.5 ml of incubation buffer (0.75 M sorbitol, 37.5 mM Tris-HCl [pH 7.5], 1.25% glucose, 6.25 mM EDTA), and 2.5 ml of freshly prepared incubation buffer containing 2.5 mg/ml (or, for the *atf1*Δ strain, 1.25 mg/ml) of Zymolyase 100T (Seikagaku Cooperation, Japan) was added and mixed well. The cells were incubated with gentle agitation at 30°C for 5 min and washed once with 5 ml of ice-cold wash buffer. The resultant spheroplasts were suspended well by pipetting in 7 ml of lysis buffer (18% Ficoll 400, 10 mM KH_2PO_4, 10 mM K_2HPO_4, 1 mM $MgCl_2$, 0.25 mM EGTA, 0.25 mM EDTA, 1 mM Pefabloc SC [Roche, Mannheim, Germany]). After centrifugation at 14,000 rpm for 30 min at 4°C, the crude nuclear pellet was resuspended in 4 ml of buffer A (10 mM Tris-HCl [pH 8.0], 150 mM NaCl, 5 mM KCl, 1 mM EDTA, 1 mM Pefabloc SC [Roche, Mannheim, Germany]). After addition of $CaCl_2$ (5 mM final concentration), 1-milliliter aliquots of crude nuclear suspension were digested with different amounts of MNase (0, 10, 20, and 50 U/ml) at 37°C for 5 min. The reaction was terminated by adding 25 mM EDTA, and DNA was purified by incubation with 1% sodium dodecyl sulfate (SDS) and 20 μg of proteinase K (Merck, Darmstadt, Germany) at 55°C followed by phenol-chloroform extraction. The DNA samples were analyzed by Southern blotting as described below. To analyze chromatin around the *tdh*$^+$, *cds1*$^+$, and *mbs1* loci, the MNase-treated DNA was digested with ApaLI/AflII, ClaI, and SpeI, respectively, and separated using agarose gel electrophoresis (40-cm-long gel) containing Tris-acetate-EDTA buffer. The separated DNA fragments were alkali transferred to charged nylon membranes (Biodyne B membrane; Pall, NY). The probe used for the indirect end labeling was prepared from PCR-amplified DNA fragments, and the DNA fragments were further labeled with ^{32}P using a random-priming kit (GE Healthcare, Little Chalfont, United Kingdom). The DNA fragments were amplified from the *S. pombe* genome by PCR using the following primer sets: for *tdh*1$^+$, CTAGCTA ATCATCCCGATG and GAGATTACACAAGACTAC; for *cds1*$^+$, GATGAT AAAGTTGATATATGGAG and GATTCCCTCTTCTGAAATTTCG; and for *mbs1*, GAATACGCGACTTAACCGC and GACGATGTGGGAGGTGTG.

ChIP. Chromatin immunoprecipitation (ChIP) was performed according to the method of Yamada et al. (40) with slight modifications as described below. Fifty milliliters of culture was incubated with 1.4 ml of 37% formaldehyde solution for 20 min at room temperature, and then 2.5 ml of 2.5 M glycine was added and incubated for 5 min. After centrifugation, collected cells were washed twice with cold Tris-buffered saline (150 mM NaCl, 20 mM Tris HCl [pH 7.5]). The cells were mixed with 400 μl of lysis 140 buffer (0.1% Na-deoxycholate, 1 mM EDTA, 50 mM HEPES-KOH [pH 7.5], 140 mM NaCl, 1% Triton X-100) supplemented with protease inhibitor cocktail (Complete Mini; Roche, Mannheim, Germany), and 0.6 ml of zirconia beads was added. After disruption of the cells using a multibead shocker (Yasuikikai, Osaka, Japan), the suspension was sonicated five times for 30 s each and centrifuged at 4°C, and the supernatant was collected as a whole-cell extract. The proper amount of antibody (anti-Flag M2; Sigma, St. Louis, MO), in accordance with the specifications provided by the manufacturer, and 40 μl of DYNA-protein G beads (DYNAL, Oslo, Norway) were mixed at 4°C overnight to conjugate antibody and beads, which were then washed twice with phosphate-buffered saline (138 mM NaCl, 2.7 mM KCl, 10 mM Na_2HPO_4, 1.8 mM KH_2PO_4) containing 0.1% bovine serum albumin. Fi-

nally, 300 μl of whole-cell extract was mixed with the pretreated beads and allowed to immunoprecipitate at 4°C overnight. The precipitates were washed twice with lysis 140 buffer, once with lysis 500 buffer (0.1% Na-deoxycholate, 1 mM EDTA, 50 mM HEPES-KOH [pH 7.5], 500 mM NaCl, 1% Triton X-100) and further washed once with wash buffer (0.5% Na-deoxycholate, 1 mM EDTA, 250 mM LiCl, 0.5% NP-40, 10 mM Tris-HCl [pH 8.0]), followed by one wash with TE buffer (10 mM Tris-HCl [pH 8.0], 1 mM EDTA). The well-washed precipitates were mixed with 150 μl of elution buffer (10 mM EDTA, 1% SDS, 50 mM Tris-HCl [pH 8.0]), and allowed to elute the immunoprecipitated protein-DNA complexes at 65°C for 15 min (IP sample). The IP sample or 3 μl of whole-cell extract was mixed with 250 μl or 397 μl of 1% SDS-containing TE buffer, 60 μg of proteinase K (Merck, Darmstadt, Germany) was added, and the mixture was incubated at 37°C for 8 h. The sample was then further incubated at 65°C overnight. The DNA present in the whole-cell extract and immunoprecipitates was purified and the DNA sample amplified by PCR using the following primer sets: for *ade6-M26*, CTCCGCACTAACTCACTAC and CGCTCATATTCGAT GAAGTATG; for *tdh1*$^+$, CGAAGCAACGACCATCTCGG and ATGCTAGG CACCGCCTGCCT; and for *mbs1*, TACGCCTCAGCGCGGAGACT and GT CAATCGCATCTACGCCTG.

The PCR products were then separated by electrophoresis, and the images were stored digitally. The amount of DNA was quantified using a Fast real-time PCR system 7300 (Applied Biosystems, Foster City, CA) and SYBER premix EX *Taq* (Takara, Japan). The IP efficiency (percent) was calculated as IP value/1% input value.

Detection of DSBs. DNA samples were prepared in agarose plugs from cells of a synchronous culture, as described by Ogino et al. (20). The plugs were thoroughly equilibrated with appropriate restriction enzyme buffer and then heated to 65°C to melt the agarose. To detect DSBs in the *tdh1*$^+$ locus, samples were held at 37°C, digested with BamHI and AflII, and separated by electrophoresis in a 1% agarose gel (40 cm long). The probe used for indirect end labeling was amplified from the *S. pombe* genome by PCR using the primer set AGCGGAG CCACGTTAC and CAATCGAGTTGGTTCATGG. When DSBs and chromatin structure were analyzed in the same gel, the restriction enzymes and probes were the same as those used in the chromatin assay described above.

RESULTS

CRE-independent natural DSBs form around a constitutively open chromatin region in *mbs1*. To examine the relationship between meiotic DSB formation and chromatin structure at natural meiotic recombination hot spots, we first analyzed the chromatin structure at the natural meiotic recombination hot spot, *mbs1*. In this analysis, we employed an indirect end-labeling analysis using partial digestion of chromatin with MNase. Because MNase preferentially digests DNA that is not wrapped on nucleosomes such as linker DNA, chromatin remodeling is detected as changes in the MNase cleavage pattern.

Because DSBs in wild-type cells are repaired promptly, they are hard to detect (1). Therefore, we used a *pat1-114 rad50s* mutant strain, which allowed us to detect DSBs efficiently. In the *rad50s* mutant strains, DSBs are not repaired, and hence they accumulate (42). The *pat1-114* allele encodes a temperature-sensitive form of Pat1 kinase, which normally serves to inhibit meiosis. Thus, when *pat1-114* strains are raised to the nonpermissive temperature, cells in culture undergo a synchronous meiosis (11, 16). A *pat1-114*-induced meiosis is generally similar to diploid wild-type meiosis in terms of meiotic recombination frequency when it is induced from G_1 phase (36). The *pat1-114* haploid cells can also undergo meiosis without affecting the timing and efficiency of meiotic DSB formation (1, 2, 6, 20, 26, 28, 29, 41, 42), although the resulting spores have low viability due to chromosome missegregation (19). Thus, synchronous meiosis using *pat1-114* is a widely used technique for analyzing DSBs in *S. pombe* (1, 2, 6, 20, 26, 28, 29, 41, 42).

To investigate the chromatin structure around DSB sites precisely, we analyzed DNA from chromatin that had been partially digested with MNase and mapped the MNase-sensitive sites. We then compared the MNase-sensitive sites with the DSB sites observed in the *pat1-114 rad50s* strain in the same gel. At the *mbs1* locus, at least three DSBs and some MNase-sensitive sites around the DSB sites were detected (Fig. 1A). The positions of the MNase-sensitive sites were unchanged in meiosis, although slight alterations in MNase sensitivity were detected at a few sites. These results suggest that DSBs are preferentially introduced around open chromatin regions at *mbs1*. The DSBs at the *mbs1* locus were detected even in the *atf1*Δ strain, but the formation of DSBs was slightly delayed and the intensity was partially reduced (wild type [6 h], 1.45% DSBs/total lane; *atf1*Δ [6 h], 0.82% DSBs/total lane [~44% reduction]). This probably reflects a partial defect in meiotic progression in *atf1*Δ strains (13, 27, 33, 37). These results suggest that the *mbs1* DSB sites are not dependent upon Atf1 (Fig. 1A).

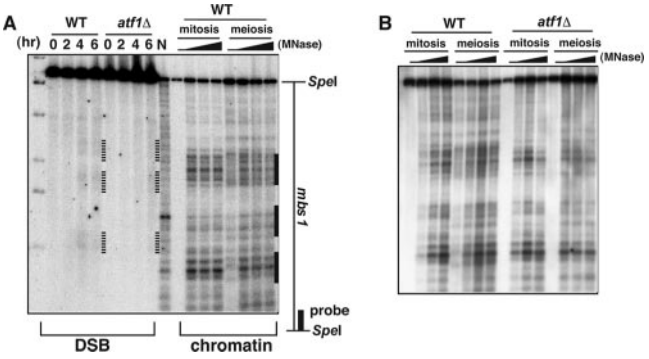

FIG. 1. The chromatin structure around the DSB sites at the *mbs1* locus shows a relatively open state in mitosis and meiosis. (A) Diploid strain D20 (wild type [WT]) was cultured in MM-NH_4Cl medium (mitosis lanes). Cells were then transferred to MM medium lacking nitrogen and cultured further for 4 h (meiosis lanes). Chromatin isolated from the cells was digested with MNase and analyzed as described previously (17). To analyze the meiotic DSBs, haploid *pat1-114 rad50s* strains PKH138 (wild type) and PKH163 (*atf1*Δ) were cultured, and DNA was prepared as described in Materials and Methods. DNA samples from MNase-digested chromatins and synchronous meioses were digested with SpeI and analyzed in the same gel. Lane N, MNase-digested naked *S. pombe* genome DNA. Meiotic DSBs are indicated by dotted lines. Thick lines indicate MNase-sensitive regions. (B) MNase-digested chromatin DNA from diploid strains D20 (wild type) and WSP779 (*atf1*Δ) were analyzed in same gel to compare the chromatin structure.

To examine the *atf1*Δ effects on the chromatin structure around *mbs1*, we next examined the pattern of MNase-sensitive sites around *mbs1* in the *atf1*Δ strain. As shown in Fig. 1B, the banding patterns of MNase-sensitive sites in the *atf1*Δ strain were similar to those in the wild type, except for slight alterations of band positions located apart from the *mbs1* DSB site. This indicates that Atf1 is dispensable for the formation of an accessible chromatin configuration around DSB sites at the *mbs1* locus (Fig. 1B). This notion is consistent with Atf1-independent DSB formation at *mbs1*.

Meiotic chromatin remodeling and Rec12-dependent DSBs are induced in the *tdh1*$^+$ locus. To test the generality of the meiotic chromatin remodeling observed at *ade6-M26*, we examined whether chromatin remodeling occurs around a natu-

TABLE 2. Meiotic chromatin remodeling in the natural *S. pombe* genome

Site[a]	Enzyme used for DNA digestion	Chromatin-remodeling region:		Constitutive open configuration <0.5 kbp from CRE sequence
		<0.5 kbp from CRE sequence	>0.5 kbp from CRE sequence	
tdh1(−334)	ApaLI/AflII	+		
cgs2(−72)	ClaI/PstI	+		
pyp2(−1147)	EcoRV/PstI		+	
cds1(+530)	ClaI			+
cgs1(−734)	SphI			+
ptc1(−190)	SphI			+
fbp1(−2737)	EcoT22I			+

[a] The position of the CRE sequence from the first ATG is indicated in parentheses.

ral CRE-related sequence in meiosis. We observed the chromatin structure at several loci containing CRE sequences (Table 2). Among them, drastic chromatin remodeling was observed at both the *tdh1*$^+$ and *cgs2*$^+$ loci in meiosis (3) (Fig. 2 and data not shown). As shown in Fig. 2, chromatin remodeling at *tdh1*$^+$ was not observed in the *atf1*Δ mutant, indicating that the chromatin remodeling in *tdh1*$^+$ requires Atf1, as in *ade6-M26*. Low levels of DNA breakages detected in meiotic samples without MNase treatment are probably due to degradation by endogenous nuclease activity in meiosis, since these breaks were independent of Rec12 around both *ade6-M26* and *tdh1*$^+$ (Fig. 3). It should be noted that meiotic chromatin remodeling was still observed in DSB-defective mutants such as the *rec12*Δ mutant, indicating that meiotic chromatin re-

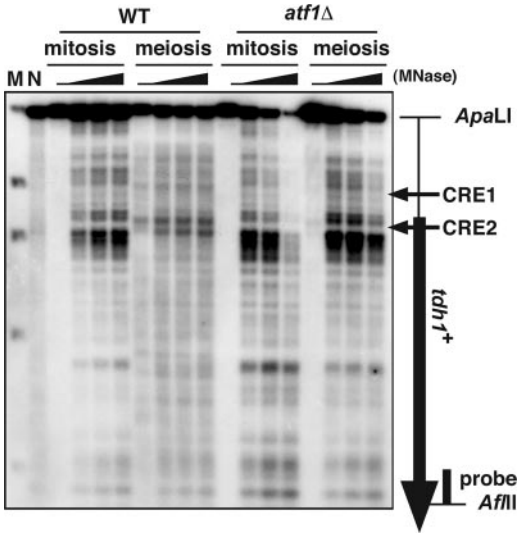

FIG. 2. Meiotic chromatin remodeling in the *tdh1*$^+$ locus depends on Atf1. MNase-digested chromatin DNAs from diploid strains D20 (wild type [WT]) and WSP779 (*atf1*Δ) were analyzed as in Fig. 1. The *atf1*Δ samples were slightly overdigested, since the *atf1*Δ mutant is more sensitive to Zymolyase treatment that allows increased permeation of MNase. The vertical and the horizontal arrows indicate the *tdh1*$^+$ ORF and the position of the CRE sequences, respectively. Lane M, marker λ, EcoT14I digested (Takara); lane N, MNase-digested naked *S. pombe* genome DNA.

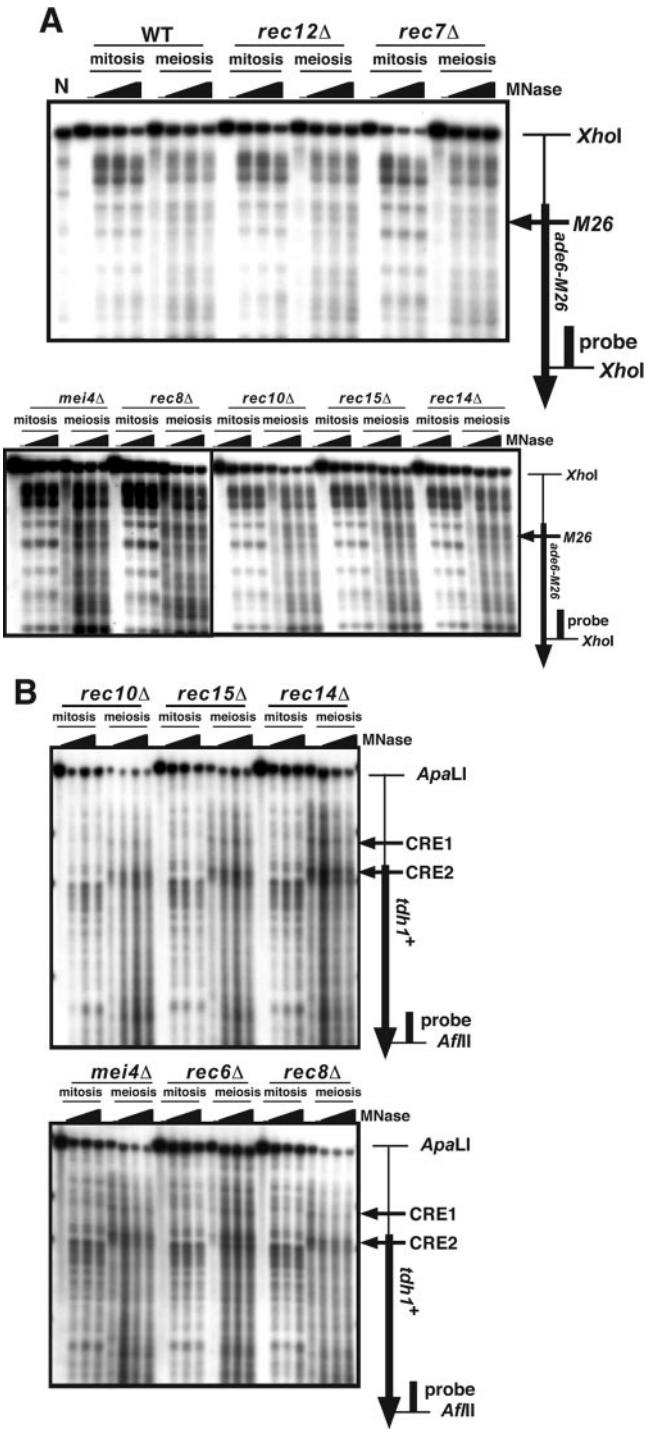

FIG. 3. The chromatin structure around *ade6-M26* and *tdh1*$^+$ in mitosis and meiosis in DSB-defective mutants. Meiotic DSB formation is critically impaired in *rec6*Δ, *rec7*Δ, *rec8*Δ, *rec10*Δ, *rec12*Δ, *rec14*Δ, *rec15*Δ, and *mei4*Δ mutants (1, 4, 6, 41). We examined the chromatin structure around *ade6-M26* (A) and *tdh1*$^+$ (B) in these mutants. The *M26* diploid strains D20 (wild type [WT]), D55 (*rec7*Δ), D68 (*rec8*Δ), D69 (*rec10*Δ), D12 (*rec12*Δ), D70 (*rec15*Δ), and D66 (*mei4*Δ) were cultured as in Fig. 1. Isolation of the chromatin fraction and treatment with MNase were done as described in Materials and Methods. Southern blot analysis was performed according to the method of Mizuno et al. (17). Lane N, partial digestion of naked DNA with MNase.

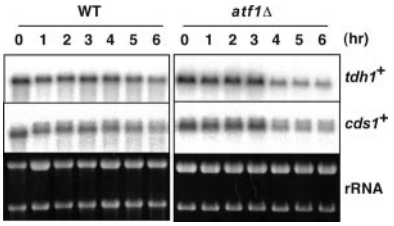

FIG. 4. The transcription of *tdh1*$^+$ and *cds1*$^+$ is not dependent on Atf1 and is not induced during meiosis. The diploid strains D20 (wild type [WT]) and WSP779 (*atf1*Δ) were cultured as in Fig. 1. The cells were harvested at the indicated time points after the medium shift. Preparation of total RNA and Northern blot analysis were performed as described in Materials and Methods. rRNA was detected by ethidium bromide staining as a loading control.

modeling precedes, and hence may be prerequisite for, meiotic DSB formation.

We previously reported that the Atf1-Pcr1-M26 complex links stress-activated mitogen-activated protein kinase and protein kinase A signaling pathways via chromatin remodeling in the *cgs2*$^+$ promoter (3). In that case, we suggested that the chromatin remodeling facilitates transcriptional activation of *cgs2*$^+$ (3). On the other hand, the transcription of *tdh1*$^+$ was not induced at all in meiosis (Fig. 4). This result led us to speculate that the chromatin remodeling in *tdh1*$^+$ is dedicated to the regulation of meiotic DSB formation. To test this notion, we next investigated DSB formation at *tdh1*$^+$. Rec12-dependent DSB formation was detected at one of the CRE sequences (CRE2) in the *tdh1*$^+$ locus at 4 h after the meiotic induction (Fig. 5A, upper panel). This meiotic DSB was not detected in the *atf1*Δ or *pcr1*Δ mutants (Fig. 5A, middle panel), while the genome-wide DSB frequency was not severely affected in those mutants (Fig. 5A, lower panel). These results indicate that meiotic DSB formation at the *tdh1*$^+$ locus is regulated by the Atf1-Pcr1 complex, as observed at *ade6-M26*.

To compare precisely the positions of the MNase-sensitive sites and DSBs, we examined them side by side on the same gel. As shown in Fig. 5B, the observed MNase-sensitive sites were located slightly downstream of the *tdh1*$^+$ DSB site in mitosis. In meiosis new MNase-sensitive sites appeared around the DSB site (Fig. 5B), and these new sites are dependent on Atf1 (Fig. 2). This result is similar to the Atf1-dependent nucleosome repositioning observed at *ade6-M26*.

The similarity between *tdh1*$^+$ and *ade6-M26* suggests that the CRE-dependent meiotic remodeling of chromatin may be a prerequisite to the loading of Rec12 and other DSB-initiating proteins onto DNA at those sites. To test this idea, we examined the binding of Rec12 protein and Rad32 (the ortholog of Mre11 in *S. pombe*) in vivo by ChIP. Both Rec12-Flag and Rad32-Flag proteins bind meiotically to *ade6-M26* but not to *ade6-M375*, which has an identical nonsense mutation at the codon adjacent to that carrying *M26* (Fig. 6A and B). We also analyzed Rec12-Flag and Rad32-Flag binding to the *tdh1*$^+$ and *mbs1* DSB sites, as natural CRE-dependent and -independent DSB hot spots, respectively. Both Rec12-Flag and Rad32-Flag proteins bind to *tdh1*$^+$ and *mbs1* during meiosis (Fig. 6A and B).

We further examined the binding of Rec12-Flag to those

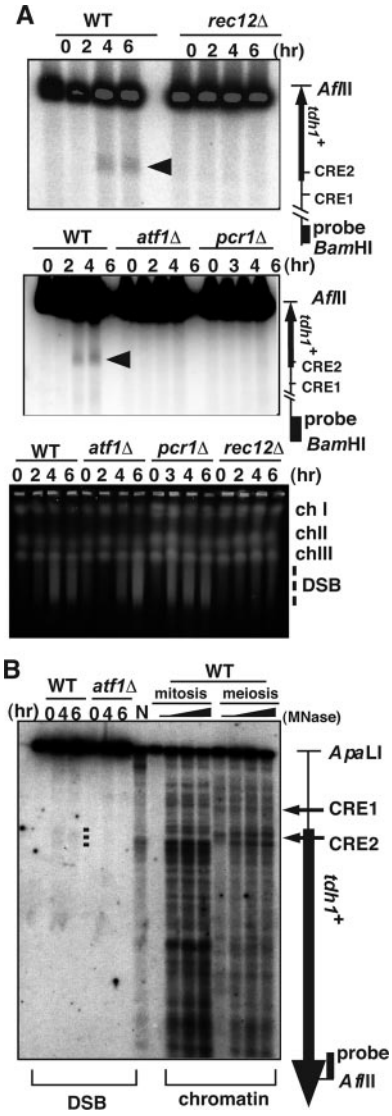

FIG. 5. Formation of meiotic DSBs in the *tdh1*$^+$ locus depends on Rec12 and the Atf1-Pcr1 complex. (A) Haploid *pat1-114 rad50s* strains PKH138 (wild type [WT]), PKH118 (*rec12*Δ), PKH163 (*atf1*Δ), and PKH160 (*pcr1*Δ) were cultured, and DNA was prepared as described in Materials and Methods. *tdh1*$^+$ ORF and CRE sequences are indicated as in Fig. 2. An arrowhead indicates the DSB site. The genome-wide DSBs in the same samples were analyzed by pulsed-field gel electrophoresis. (B) DNA samples from the MNase-digested chromatins and synchronous meioses in Fig. 1 were digested with ApaLI and AflII and analyzed in the same gel. DSBs are indicated by a dotted line; *tdh1*$^+$ ORF and CRE sequences are indicated as in Fig. 2.

DSB sites in the *atf1*Δ mutant, in which cellular CRE-mediated chromatin remodeling may be impaired. The binding of Rec12-Flag to *ade6-M26* and *tdh1*$^+$ was reduced five- to sevenfold relative to that in the *atf1*$^+$ strain (Fig. 6C and D). On the other hand, the binding of Rec12-Flag to *mbs1* was reduced only ~2.7-fold. Notably, the Rec12-Flag binding to *mbs1* increased 5.6-fold between 4 and 6 h of meiosis. Thus, the Rec12-Flag binding at *mbs1* is partly reduced and delayed in the *atf1*Δ mutant, but the levels are still higher than those in the Atf1-dependent hot spots, *ade6-M26* and *tdh1*$^+$ (Fig. 6C

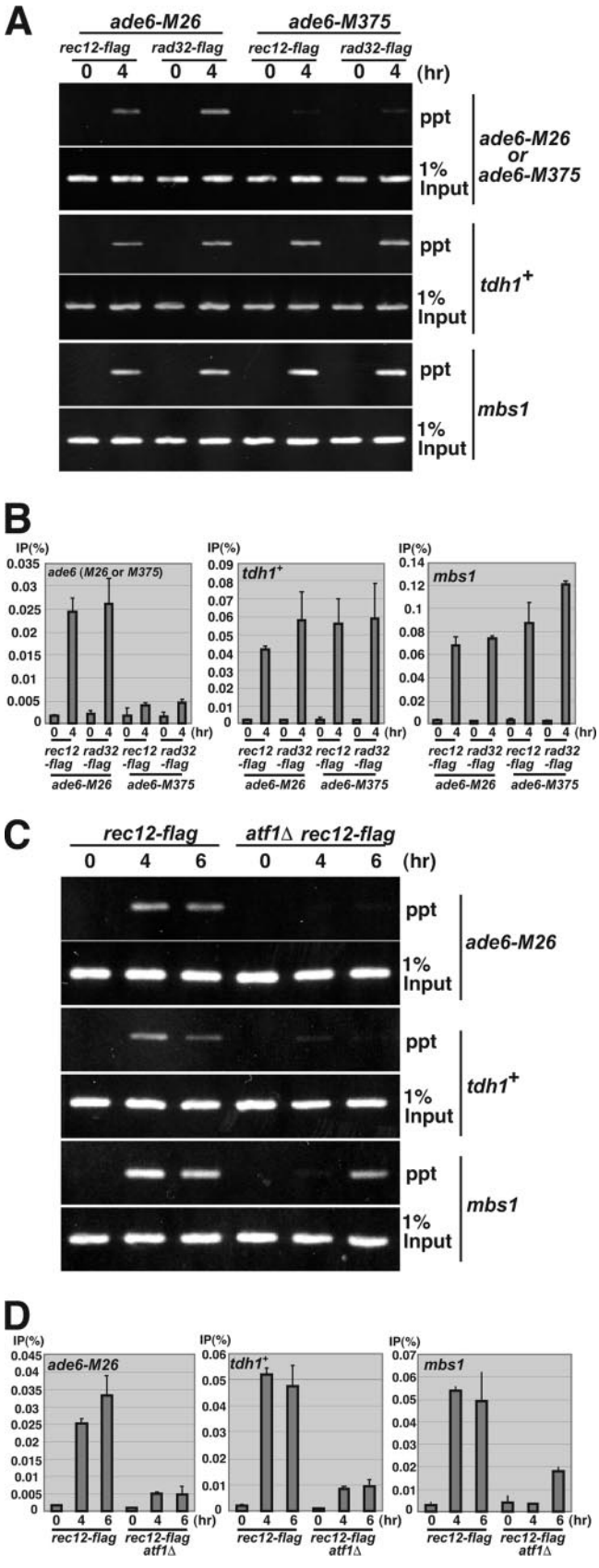

and D). It is likely that the reduced and delayed DSB formation at *mbs1* in the *atf1*Δ mutant is due to its impaired ability to proceed through meiosis. From these data, we conclude that Atf1-CRE-mediated chromatin alteration is a prerequisite for the binding of DSB-initiating proteins to DNA at *ade6-M26* and *tdh1*$^+$ but not at *mbs1*.

Chromatin structure around the *cds1*$^+$ locus exhibits an Atf1-dependent constitutively open configuration. In an independent study, it was demonstrated that natural meiotic DSB sites occur at many CRE-like sequences present naturally in the *S. pombe* genome (29). One of the prominent DSB sites, the *cds1*$^+$ locus, was demonstrated to be an Atf1-Pcr1-dependent meiotic recombination hot spot (29). We analyzed the chromatin structure around the *cds1*$^+$ locus and compared it to the observed DSB site (Fig. 7A). Surprisingly, MNase sensitivity was high at the CRE sequence, and the MNase cleavage patterns appeared to be virtually identical in mitosis and meiosis. In addition, the meiosis-specific DSBs observed at *cds1*$^+$ occur adjacent to a site that is constitutively accessible in mitosis and meiosis.

Because DSB formation is dependent on the Atf1-Pcr1 complex in *cds1*$^+$ (29) (Fig. 7A), we also analyzed chromatin structure in the *atf1*Δ mutant. Interestingly, the MNase cleavage sites around the DSB sites were abolished in both mitotic and meiotic chromatin by the *atf1*Δ mutation, indicating that formation of the open chromatin configuration in *cds1*$^+$ depends on the Atf1 protein (Fig. 7B). In addition, we monitored the transcription of *cds1*$^+$ during meiosis in the wild-type and *atf1*Δ strains. The expression of *cds1*$^+$ was not induced during meiosis irrespective of presence or absence of Atf1, indicating that Atf1 bound on that site does not participate in the regulation of *cds1*$^+$ transcription (Fig. 4). We also analyzed the chromatin structure at *cds1-2*, a point mutation that abolishes the CRE sequence in the *cds1* gene (29). The chromatin structure around the *cds1-2* mutation showed reduced accessibility compared to *cds1*$^+$ in mitosis, and the accessibility was further reduced in meiosis (Fig. 7). Thus, it is likely that the role of Atf1 at this locus is to maintain a constitutively open chromatin

FIG. 6. Rec12 and Rad32 proteins bind to meiotic DSB sites *ade6-M26*, *tdh1*$^+$ (CRE-mediated hot spots), and *mbs1* (CRE-independent hot spot) in meiosis. (A) The binding of Rec12-Flag and Rad32-Flag proteins to the *ade6* locus carrying the *M26* or *M375* allele was examined. The haploid *pat1-114 rad50s* strains PKH50 (*rec12-flag ade6-M26*), PKH52 (*rad32-flag ade6-M26*), PKH338 (*rec12-flag ade6-M375*), and PKH339 (*rad32-flag ade6-M375*) were cultured to induce meiosis (0 and 4 h) and fixed with formaldehyde. ChIP analysis was performed as described in Materials and Methods. The binding of Rec12-Flag and Rad32-Flag to the *ade6*, *tdh1*$^+$, and *mbs1* loci was detected using PCR. Whole genomic DNA from the 1% input sample was amplified at the same time. (B) ChIP efficiency in the *M26* and *M375* alleles was quantified by real-time PCR analysis as described in Materials and Methods. ChIP efficiency was calculated as IP sample/input material and represented as IP (percent) Error bars represent standard deviations. (C) The binding of Rec12-Flag protein to the *ade6*, *tdh1*$^+$, and *mbs1* loci was examined in wild-type and *atf1*Δ strains. The haploid *ade6-M26 pat1-114 rad50s rec12-flag* strains PKH50 (wild type) and PKH114 (*atf1*Δ) were cultured to induce meiosis (0, 4, and 6 h) and fixed with formaldehyde. The binding of Rec12-Flag to *ade6*, *tdh1*$^+$, and *mbs1* loci was detected as for panel A. (D) Quantification of ChIP efficiency from panel C. Error bars represent standard deviations.

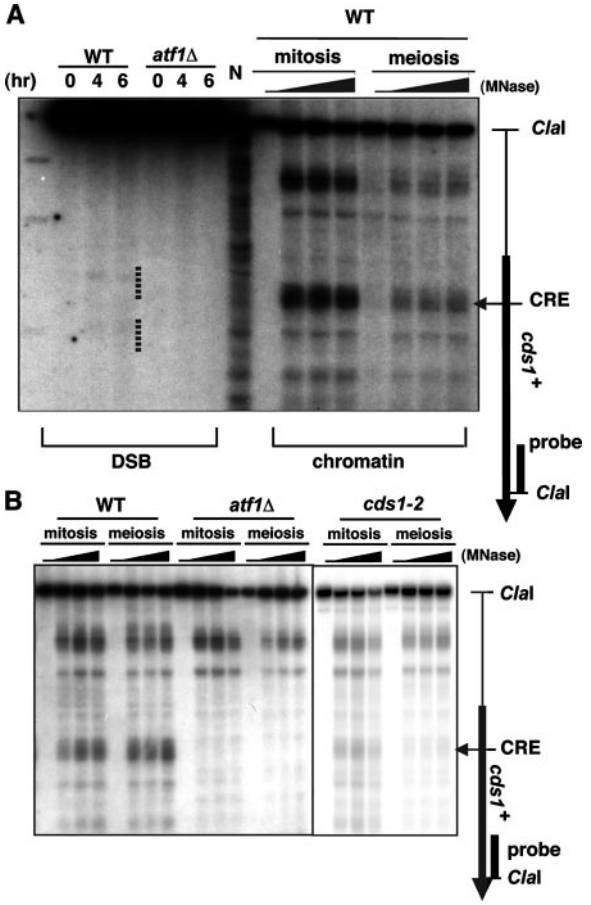

FIG. 7. The chromatin structure at the CRE sequence in the *cds1*$^+$ locus demonstrates a constitutively open state in an Atf1-dependent manner. (A) Meiotic DSB and chromatin structures were analyzed in the same gel. The ORF of *cds1*$^+$ and its associated CRE sequence are indicated as in Fig. 2. Lane N, MNase-digested naked *S. pombe* genome DNA. Meiotic DSBs are indicated by dotted lines. (B) The chromatin structures in diploid strains D20 (wild type [WT]), WSP779 (*atf1*Δ), and D74 (*cds1-2*) were compared as for Fig. 1. The CRE sequence is indicated by an arrowhead.

configuration during mitosis and meiosis, rather than to induce an alteration in chromatin configuration as observed in *ade6-M26* (29).

DISCUSSION

This study provides the first evidence that chromatin remodeling occurs in meiosis at natural meiotic DSB sites in *S. pombe*. In addition, we demonstrated that CRE-dependent DSB sites also show a CRE-dependent (or Atf1-Pcr1-dependent) open chromatin configuration. The open chromatin configuration at these sites may be constitutive (*cds1*$^+$) or meiotically induced (*tdh1*$^+$).

The regulation pattern of the chromatin configuration in natural meiotic recombination hot spots can be classified into at least three types. We analyzed meiotic DSB formation at three distinct chromosomal loci and found that DSBs at those loci occur around regions with an open chromatin configuration. The chromatin structure around the DSB sites of *mbs1* is accessible and changes little from mitosis to meiosis (Fig. 1). Chromatin around the CRE2 site of *tdh1*$^+$ also shows an open chromatin configuration in mitosis, but significant Atf1-dependent chromatin remodeling is observed there during meiosis (Fig. 2). Chromatin at the CRE site of *cds1*$^+$ has a constitutive open configuration, but unlike *mbs1*, this open chromatin configuration is dependent on Atf1 (Fig. 7). These results indicate that there are at least three types of regulation of chromatin configuration around meiotic DSB sites: (i) an Atf1-CRE-independent constitutively open chromatin configuration (*mbs1*), (ii) an Atf1-CRE-mediated meiotic chromatin alteration to a more accessible configuration (*tdh1*$^+$), and (iii) an Atf1-CRE-dependent constitutively accessible chromatin configuration (*cds1*$^+$). At those sites tested in *S. cerevisiae*, meiotic DSBs are formed around sites with a constitutively open chromatin configuration, such as the well-characterized DSB sites *ARG4* and *CYC3* (21). On the other hand, the results in this study suggest that the situation in *S. pombe* is more complex; e.g., meiotic DSB sites show distinct modes of chromatin configuration before meiotic DSB formation.

General roles of ATF1-CRE dependent chromatin alteration in meiotic recombination in *S. pombe*. The *S. pombe* genome has number of CRE-related Atf1-dependent meiotic DSB sites (29). In this study, we report that *tdh1*$^+$ is also an Atf1-CRE-dependent DSB site (Fig. 5). We further demonstrate that Atf1-dependent chromatin remodeling (i.e., changes in MNase-sensitive sites) occurs during meiosis around the DSB site in the *tdh1*$^+$ locus (Fig. 2 and 5). In addition, the *atf1*Δ mutation severely affects meiotic chromatin remodeling in *tdh1*$^+$, DSB formation, and the binding of DSB initiating proteins in *tdh1*$^+$ (Fig. 2, 5, and 6), Thus, the regulation of chromatin structure and recombination at *tdh1*$^+$ is very similar to the artificial CRE-dependent hot spot *ade6-M26* (17).

The DSB site found in the *cds1*$^+$ locus is another CRE-Atf1-dependent recombination hot spot (29). However, unlike *ade6-M26* and *tdh1*$^+$, the *cds1*$^+$ locus shows an Atf1-dependent constitutively open configuration at the CRE site in both mitosis and meiosis (Fig. 7). Interestingly, mutation of the CRE sequence (*cds1-2*) results in a significant reduction in MNase sensitivity at that site in mitosis and an even greater reduction in meiosis (Fig. 7B). In meiosis, the chromatin configuration around the CRE consensus sequence in *cds1-2* is very similar to that of the *cds1*$^+$ *atf1*Δ mutant in meiosis. It is unclear why the *cds1-2* mutant shows a partially open configuration in mitotic cells, but a residual binding of Atf1 to the mutated CRE sequence may be sufficient to form the partially open chromatin configuration in mitotic cells but not in meiotic cells. Alternatively, another CRE-related site, ~350 bp upstream of the *cds1-2* CRE, may contribute to the open chromatin configuration in mitosis but not in meiosis.

Formation of accessible chromatin is pivotal for the binding of DSB-initiating proteins to DSB sites in meiosis. We demonstrated that Rec12 and Rad32 (the orthologs of Spo11 and Mre11 in *S. pombe*, respectively) bind to the *ade6-M26* DSB site in meiosis (Fig. 6). Importantly, such binding of Rec12 and Rad32 to the *ade6* locus is not observed in *ade6-M375*, a negative control allele. Moreover, we showed that Atf1 is required for the binding of Rec12 to *ade6-M26* and *tdh1*$^+$ (Fig. 6C and D). Since the alteration of chromatin structure is dependent on the CRE-Atf1 complex (15, 37), these results suggest that the

M26 meiotic chromatin alteration may be pivotal for the binding of DSB-initiating proteins to DSB sites. An alternative but nonexclusive possibility is that Atf1 directly recruits Rec12 together with other DSB-initiating proteins to CRE-related sites, and then the chromatin alteration occurs as a consequence of the binding of those proteins. However, this notion seems unlikely, since the binding of DSB-initiating proteins to DSB sites is severely reduced in another type of chromatin alteration-defective mutants, *hsk1-89*, a temperature-sensitive allele of *hsk1*$^+$ encoding the fission yeast *CDC7* homolog (K. Hirota et al., unpublished results) (20, 32). In addition, at the *ade6-M26* and *tdh1*$^+$ loci, the chromatin remodeling is observed even in mutants lacking *rec12*$^+$ and other genes (*rec7*$^+$, *rec10*$^+$, *rec14*$^+$, *rec15*$^+$, *mei4*$^+$, and *rec8*$^+$) involved in DSB formation (Fig. 3). From these results, we propose that meiotic chromatin remodeling is prerequisite for, but not a consequence of, the binding of DSB-initiating proteins at those sites.

Biological significance of CRE-related meiotic recombination and chromatin alteration. We speculate that CRE-dependent meiotic recombination may account for a small portion of the total recombination events occurring in *S. pombe*, since the maximum frequency of whole DSBs is generally unaffected in *atf1*Δ or *pcr1*Δ strains (Fig. 5). Although their contribution may be limited, it is possible that Atf1-CRE-mediated meiotic recombination is conserved in other eukaryotes in which the Atf1-CRE-type transcriptional regulation units are present. Thus, it is possible that the Atf1-CRE complex acts as an additional regulatory level for meiotic recombination, in addition to its function as a transcription factor. Further investigation of CRE-related meiotic recombination hot spots may enlarge the definition of "CRE-dependent transcription factors".

ACKNOWLEDGMENTS

K.H. thanks all members of the Genetic System Regulation Laboratory and Cellular and Molecular Biology Laboratory in Riken for helpful discussion and K. Ogino and H. Masai for the *hsk1-89* strain of fission yeast. We thank T. Yamada for critical advice regarding ChIP analysis. We also thank Y. Ichikawa and R. Nakazawa for DNA sequencing and Y. Sakuma for technical assistance.

This work was supported by basic research grants from the Bio-oriented Technology Research Advancement Institution (to T. Shibata and K. Ohta) and by grants-in-aid for scientific research on priority areas from the Ministry of Education, Science, Culture, & Sports, Japan (to K. Ohta). Walter Steiner was supported by a special fellowship (3230-05) from the Leukemia and Lymphoma Society and a grant (GM078065) from the National Institutes of Health.

REFERENCES

1. **Cervantes, M. D., J. A. Farah, and G. R. Smith.** 2000. Meiotic DNA breaks associated with recombination in *S. pombe*. Mol. Cell **5:**883–888.
2. **Cromie, G. A., C. A. Rubio, R. W. Hyppa, and G. R. Smith.** 2005. A natural meiotic DNA break site in *Schizosaccharomyces pombe* is a hotspot of gene conversion, highly associated with crossing over. Genetics **169:**595–605.
3. **Davidson, M. K., H. K. Shandilya, K. Hirota, K. Ohta, and W. P. Wahls.** 2004. Atf1-Pcr1-M26 complex links stress-activated MAPK and cAMP-dependent protein kinase pathways via chromatin remodeling of *cgs2*+. J. Biol. Chem. **279:**50857–50863.
4. **Davis, L., and G. R. Smith.** 2001. Meiotic recombination and chromosome segregation in *Schizosaccharomyces pombe*. Proc. Natl. Acad. Sci. USA **98:** 8395–8402.
5. **Elder, R. T., E. Y. Loh, and R. W. Davis.** 1983. RNA from the yeast transposable element Ty1 has both ends in the direct repeats, a structure similar to retrovirus RNA. Proc. Natl. Acad. Sci. USA **80:**2432–2436.
6. **Ellermeier, C., and G. R. Smith.** 2005. Cohesins are required for meiotic DNA breakage and recombination in *Schizosaccharomyces pombe*. Proc. Natl. Acad. Sci. USA **102:**10952–10957.
7. **Fan, Q., F. Xu, and T. D. Petes.** 1995. Meiosis-specific double-strand DNA breaks at the *HIS4* recombination hot spot in the yeast *Saccharomyces cerevisiae*: control in *cis* and *trans*. Mol. Cell. Biol. **15:**1679–1688.
8. **Gutz, H.** 1971. Site specific induction of gene conversion in *Schizosaccharomyces pombe*. Genetics **69:**317–337.
9. **Gutz, H., H. Heslot, U. Leupold, and N. Loprieno.** 1974. *Schizosaccharomyces pombe*, p. 395–446. *In* R. D. King (ed.), Handbook of genetics, vol. 1. Plenum, New York, NY.
10. **Hirota, K., K. Tanaka, Y. Watanabe, and M. Yamamoto.** 2001. Functional analysis of the C-terminal cytoplasmic region of the M-factor receptor in fission yeast. Genes Cells **6:**201–214.
11. **Iino, Y., and M. Yamamoto.** 1985. Negative control for the initiation of meiosis in *Schizosaccharomyces pombe*. Proc. Natl. Acad. Sci. USA **82:**2447–2451.
12. **Isshiki, T., N. Mochizuki, T. Maeda, and M. Yamamoto.** 1992. Characterization of a fission yeast gene, gpa2, that encodes a G alpha subunit involved in the monitoring of nutrition. Genes Dev. **6:**2455–2462.
13. **Kanoh, J., Y. Watanabe, M. Ohsugi, Y. Iino, and M. Yamamoto.** 1996. *Schizosaccharomyces pombe gad7*+ encodes a phosphoprotein with a bZIP domain, which is required for proper G1 arrest and gene expression under nitrogen starvation. Genes Cells. **1:**391–408.
14. **Kon, N., M. D. Krawchuk, B. G. Warren, G. R. Smith, and W. P. Wahls.** 1997. Transcription factor Mts1/Mts2 (Atf1/Pcr1, Gad7/Pcr1) activates the M26 meiotic recombination hotspot in *Schizosaccharomyces pombe*. Proc. Natl. Acad. Sci. USA **94:**13765–13770.
15. **Lichten, M., and A. S. Goldman.** 1995. Meiotic recombination hotspots. Annu. Rev. Genet. **29:**423–444.
16. **McLeod, M., and D. Beach.** 1986. Homology between the *ran1*+ gene of fission yeast and protein kinases. EMBO J. **5:**3665–3671.
17. **Mizuno, K., Y. Emura, M. Baur, J. Kohli, K. Ohta, and T. Shibata.** 1997. The meiotic recombination hot spot created by the single-base substitution *ade6-M26* results in remodeling of chromatin structure in fission yeast. Genes Dev. **11:**876–886.
18. **Nachman, M. W.** 2002. Variation in recombination rate across the genome: evidence and implications. Curr. Opin. Genet. Dev. **12:**657–663.
19. **Nurse, P.** 1985. Mutants of the fission yeast *Schizosaccharomyces pombe* which alter the shift between cell proliferation and sporulation. Mol. Gen. Genet. **198:**497–502.
20. **Ogino, K., K. Hirota, S. Matsumoto, T. Takeda, K. Ohta, K. Arai, and H. Masai.** 2006. Hsk1 kinase is required for induction of meiotic dsDNA breaks without involving checkpoint kinases in fission yeast. Proc. Natl. Acad. Sci. USA **103:**8131–8136.
21. **Ohta, K., T. Shibata, and A. Nicolas.** 1994. Changes in chromatin structure at recombination initiation sites during yeast meiosis. EMBO J. **13:**5754–5763.
22. **Petes, T. D.** 2001. Meiotic recombination hot spots and cold spots. Nat. Rev. Genet. **2:**360–369.
23. **Ponticelli, A. S., E. P. Sena, and G. R. Smith.** 1988. Genetic and physical analysis of the M26 recombination hotspot of Schizosaccharomyces pombe. Genetics **119:**491–497.
24. **Sambrook, J., E. F. Fritsch, and T. Maniatis.** 1989. Molecular cloning: a laboratory manual, 2nd ed. Cold Spring Harbor Laboratory Press, Cold Spring Harbor, NY.
25. **Schuchert, P., M. Langsford, E. Kaslin, and J. Kohli.** 1991. A specific DNA sequence is required for high frequency of recombination in the *ade6* gene of fission yeast. EMBO J. **10:**2157–2163.
26. **Shimada, M., K. Nabeshima, T. Tougan, and H. Nojima.** 2002. The meiotic recombination checkpoint is regulated by checkpoint rad+ genes in fission yeast. EMBO J. **21:**2807–2818.
27. **Shiozaki, K., and P. Russell.** 1996. Conjugation, meiosis, and the osmotic stress response are regulated by Spc1 kinase through Atf1 transcription factor in fission yeast. Genes Dev. **10:**2276–2288.
28. **Steiner, W. W., R. W. Schreckhise, and G. R. Smith.** 2002. Meiotic DNA breaks at the *S. pombe* recombination hot spot *M26*. Mol. Cell **9:**847–855.
29. **Steiner, W. W., and G. R. Smith.** 2005. Natural meiotic recombination hot spots in the *Schizosaccharomyces pombe* genome successfully predicted from the simple sequence motif *M26*. Mol. Cell. Biol. **25:**9054–9062.
30. **Sun, H., D. Treco, N. P. Schultes, and J. W. Szostak.** 1989. Double-strand breaks at an initiation site for meiotic gene conversion. Nature **338:**87–90.
31. **Szankasi, P., W. D. Heyer, P. Schuchert, and J. Kohli.** 1988. DNA sequence analysis of the *ade6* gene of *Schizosaccharomyces pombe*. Wild-type and mutant alleles including the recombination host spot allele *ade6-M26*. J. Mol. Biol. **204:**917–925.
32. **Takeda, T., K. Ogino, K. Tatebayashi, H. Ikeda, K. Arai, and H. Masai.** 2001. Regulation of initiation of S phase, replication checkpoint signaling, and maintenance of mitotic chromosome structures during S phase by Hsk1 kinase in the fission yeast. Mol. Biol. Cell **12:**1257–1274.
33. **Takeda, T., T. Toda, K. Kominami, A. Kohnosu, M. Yanagida, and N. Jones.** 1995. *Schizosaccharomyces pombe atf1*+ encodes a transcription factor required for sexual development and entry into stationary phase. EMBO J. **14:**6193–6208.

34. **Wahls, W. P.** 1998. Meiotic recombination hotspots: shaping the genome and insights into hypervariable minisatellite DNA change. Curr. Top. Dev. Biol. **37:**37–75.
35. **Wahls, W. P., and G. R. Smith.** 1994. A heteromeric protein that binds to a meiotic homologous recombination hot spot: correlation of binding and hot spot activity. Genes Dev. **8:**1693–1702.
36. **Watanabe, Y., S. Yokobayashi, M. Yamamoto, and P. Nurse.** 2001. Premeiotic S phase is linked to reductional chromosome segregation and recombination. Nature **409:**359–363.
37. **Wilkinson, M. G., M. Samuels, T. Takeda, W. M. Toone, J. C. Shieh, T. Toda, J. B. Millar, and N. Jones.** 1996. The Atf1 transcription factor is a target for the Sty1 stress-activated MAP kinase pathway in fission yeast. Genes Dev. **10:**2289–2301.
38. **Wolffe, A.** 1997. Chromatin: structure and function, 3rd ed. Academic Press, San Diego, CA.
39. **Wu, T. C., and M. Lichten.** 1994. Meiosis-induced double-strand break sites determined by yeast chromatin structure. Science **263:**515–518.
40. **Yamada, T., K. I. Mizuno, K. Hirota, N. Kon, W. P. Wahls, E. Hartsuiker, H. Murofushi, T. Shibata, and K. Ohta.** 2004. Roles of histone acetylation and chromatin remodeling factor in a meiotic recombination hotspot. EMBO J. **23:**1792–1803.
41. **Young, J. A., R. W. Hyppa, and G. R. Smith.** 2004. Conserved and nonconserved proteins for meiotic DNA breakage and repair in yeasts. Genetics **167:**593–605.
42. **Young, J. A., R. W. Schreckhise, W. W. Steiner, and G. R. Smith.** 2002. Meiotic recombination remote from prominent DNA break sites in *S. pombe*. Mol. Cell **9:**253–263.